THE EFFECT OF COLUMN SHAPE ON LINEAR DIFFRACTION EFFECTS

J.R. Grice , P.H. Taylor , A.G.L. Borthwick, D.A.G. Walker[1] & R. Eatock Taylor

Department of Engineering Science, University of Oxford, UK
[1]Now at BP Exploration Operating Co. Ltd, UK

1 INTRODUCTION

This paper discusses the interaction of linear regular waves with bottom-seated columns, both isolated and in arrays. Much work has been carried out to understand the influence of size and relative positions of circular cylinders on the diffraction effects observed for linear incident regular waves (McIver (1984), Evans and Porter (1997), Walker et al. (2008)) but this paper investigates how dependent interaction effects are on the cross-sectional shape of the columns. Offshore structures often face large waves which can lead to water impact at deck level creating a risk for both personnel and equipment. A better understanding of how waves interact with arrays of surface piercing columns can help minimise these risks.

Both run-up on the columns and upwelling in the surrounding area were calculated for two column shapes: circular and square with rounded edges using the well validated numerical diffraction code, DIFFRACT, which utilises the Boundary Element Method. These numerical simulations were run at wavenumbers and wave directions corresponding with near-trapping modes for a particular case of the circular cylinders in a square array.

2 SINGLE COLUMN

Figure 1 shows run-up plotted against wavenumber for both circular and non-circular single bottom-seated columns with unit amplitude incident waves, a water depth of d/a=2.43 (a is the circular radius) and a wavenumber range of ka=0-9. The cross-sections are shown in Figure 1 inset and the average cross-sectional area of each column is the same with the wavenumber normalised by the circular radius for all cases.

The solid bold line represents the maximum possible run-up amplification relative to the incident amplitude on the circular cylinder. This begins at 1 for a wavenumber of zero and rises to an asymptote of 2 for very short waves

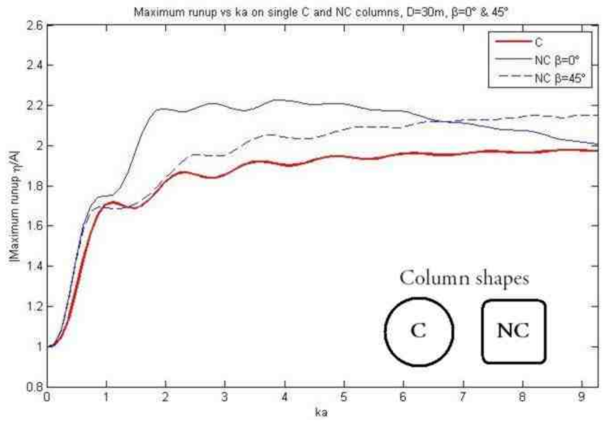

Figure 1: |Maximum run-up| on single circular (C) and non-circular (NC) columns for ka = 0-9 (where a is the circular radius)

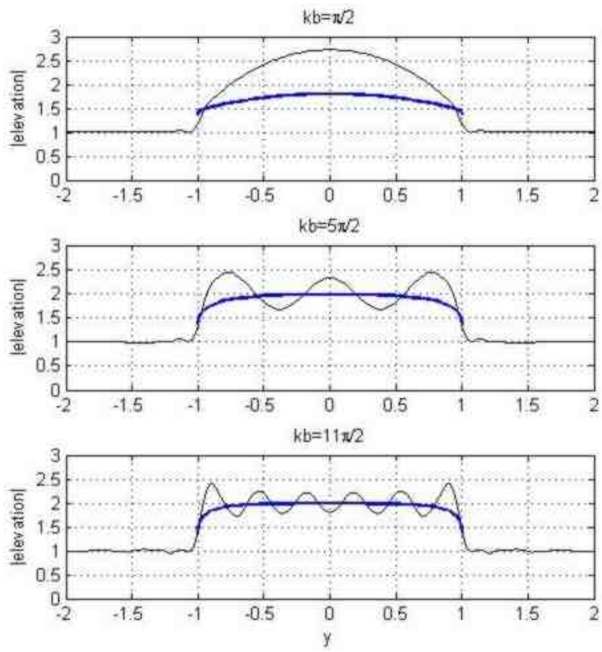

Figure 2: Run-up on a flat plate of width $2b$ (thin line) and on an equivalent circular cylinder (bold line) for $kb = \pi/2$, $5\pi/2$ & $11\pi/2$

with small oscillations about the general trend. As the wavenumber increases, the wavelength becomes small relative to the cylinder diameter and the cylinder can eventually be locally approximated as a flat wall. The amplification is then the sum of the incident and reflected wave, giving the asymptote of 2.

The thin solid and dashed lines show the maximum possible run-up at any point on the non-circular cylinder for $\beta = 0°$ and $\beta = 45°$ wave directions respectively (where $\beta = 0°$ is positive along the x axis and perpendicular to a flat face). For the non-circular $\beta = 0°$ case the maximum run-up increases much faster with wavenumber than for the circular cylinder, first reaching an amplification of 2.2 at ka=1.74 and then it slowly asymptotes down to 2 with small oscillations about the trend. For the non-circular $\beta = 45°$ case the maximum run-up increases only a little faster than for the circular case. The maximum value reached, 2.15, is not as high as for the $\beta = 0°$ case, 2.23.

The reason the maximum amplification on the non-circular cylinders is higher than for the circular cylinder is due to Fresnel diffraction effects. Figure 2 shows the run-up on a vertical flat plate of width $2b$ (thin line), positioned perpendicular to flow in a channel and the run-up on a vertical circular cylinder of the same dimensions (bold line). The equations used for run-up on the plate are based on those derived by Molin et al (2007). These figures not only show run-up on the plate in excess of the asymptote of 2 but also significant variation along the length of the plate. It can be seen that as the wavenumber increases the variation along the plate about a run-up value of 2 decreases in amplitude. The run-up on the circular cylinder is plotted against position on the y axis and the oscillations seen along the plate are not seen around the circular cylinder. Previous work by Molin et al. (2005) showed that similar first order effects to those shown above on the plate were also present on a square cylinder by calculating run-up using both a Boussinesq model and WAMIT.

Field plots show that the shape of the column can cause significant changes to the diffracted field for several diameters out from the column. Figures 3(a) and 3(b) show comparisons of the circular and non-circular columns discussed above for a regular wave with $\beta = 0°$ & ka=1.831, which is in the range of ka values that shows a large difference between the run-up on the two column shapes.

There is little difference in the general pattern caused by single circular and non-circular columns at either wave direction. However the amplitudes within the general pattern are modified with notably higher run-up on the non-circular cylinder for the $\beta = 0°$ wave direction. There are maximum values of 2.17 and 1.87 respectively, giving a 16% increase with the non-circular geometry, and also increased amplification for several diameters' distance upstream. For the $\beta = 45°$ wave direction (Figures 3(c) and 3(d)) there is reduced run-up on the non-circular cylinder with a maximum value of 1.79 compared to 1.87. The location of the maximum run-up was not on the leading rounded edge but to the side on the adjacent flat faces. There is also reduced amplification upstream and increased elevation downstream relative to the circular case.

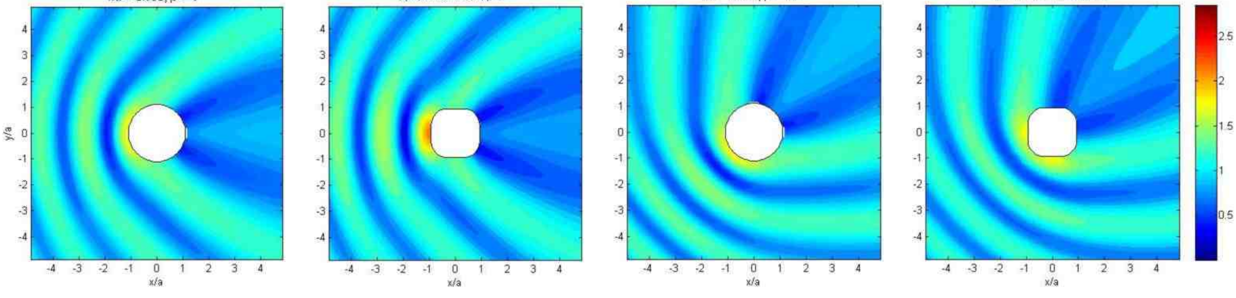

(a) C cylinder, $\beta = 0°$ (b) NC cylinder, $\beta = 0°$ (c) C cylinder, $\beta = 45°$ (d) NC cylinder, $\beta = 45°$

Figure 3: Scattered surface elevation amplitude around one bottom-seated circular (C) or non-circular (NC) column for ka=1.831

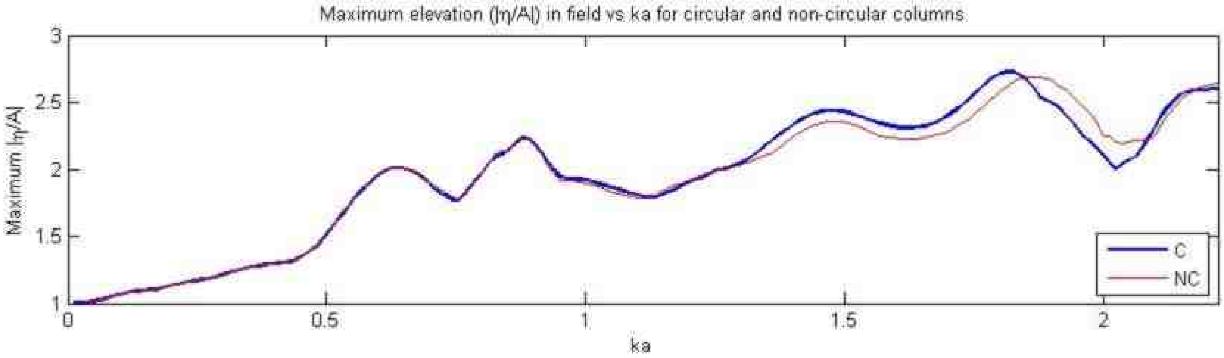

Figure 4: Maximum elevation anywhere in field vs ka for circular, (C) and non-circular, (NC) columns with $\beta = 45°$

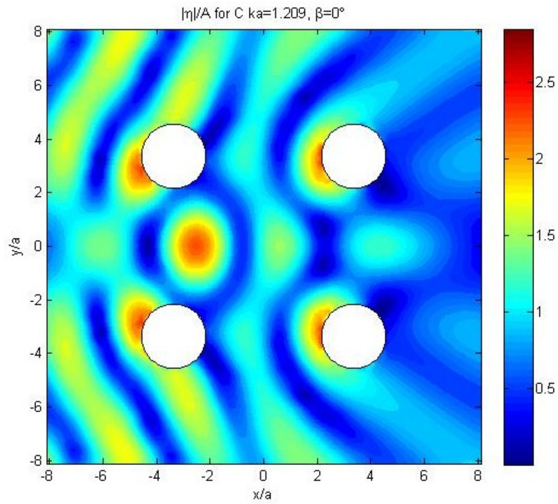

(a) Circular cylinders, $\beta = 0°$, ka=1.209

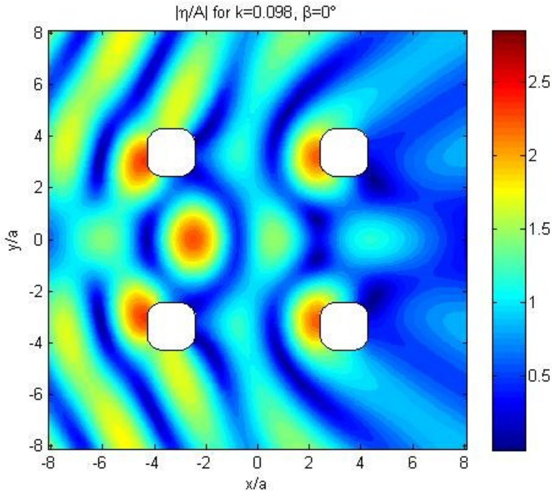

(b) Non-circular cylinders, $\beta = 0°$, ka=1.209

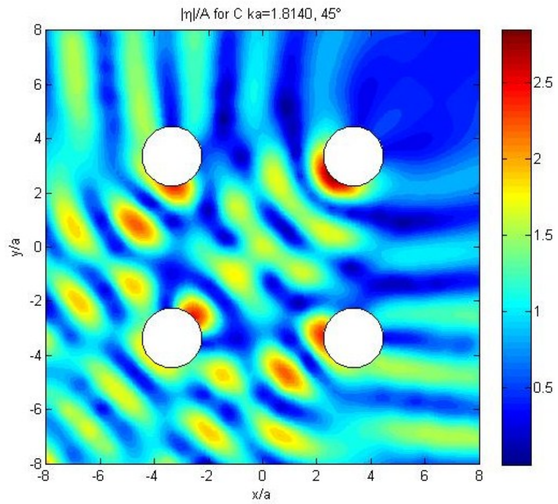

(c) Circular cylinders, $\beta = 45°$, ka_C=1.814

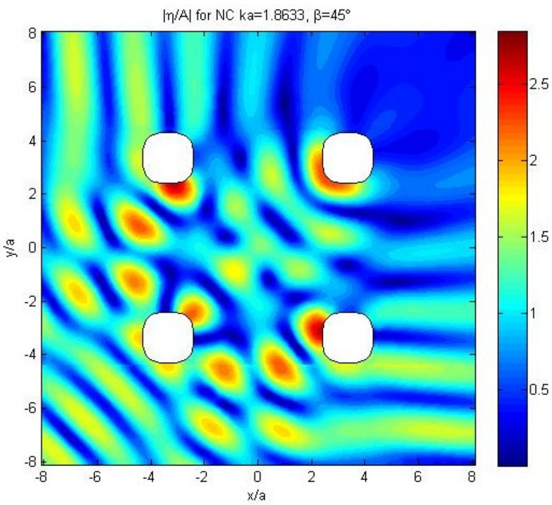

(d) Non-circular cylinders, $\beta = 45°$, ka_{NC}=1.863

Figure 5: Scattered surface elevation amplitude around four bottom-seated columns for $\beta = 0°$, ka=1.209 & $\beta = 45°$, ka_C=1.814, ka_{NC}=1.863 where a is the circular radius

3 ARRAYS OF COLUMNS

The figures from the previous section show that shape does affect the diffraction caused by a single cylinder but the effect of column shape on the interaction with arrays is of more interest to us.

For a comparison between the circular and non-circular column shape discussed above, field plots of surface elevation were calculated for each case using near-trapping frequencies for four circular cylinders (the geometries are shown in Fig. 5). Figure 4 shows the maximum amplification anywhere in the field versus ka for circular and non-circular geometries with a wave direction of $\beta = 45°$. For low ka values, column shape has very little effect on the maximum values with the plots being almost identical. As ka gets larger there is more deviation between the plots in the peak frequencies and their associated magnitudes.

Figure 5 shows diffraction around a square array of four bottom-seated columns with the cross-sections as discussed above, a centre-centre spacing, $2h$/a=6.71, a water depth, d/a=2.43 and incident waves of unit amplitude. The ka values of the regular incident waves are ka=1.209 for both geometries with $\beta = 0°$ and ka_C =1.8140 and ka_{NC} =1.8633 for $\beta = 45°$. The $\beta = 0°$ cases are both at a near-trapping frequency for the circular geometry, showing how the column shape effects the magnitude of the elevations. The $\beta = 45°$ cases are each at an equivalent near-trapping mode with ka values specific to their geometry. Each near-trapping frequency, Evans & Porter (1997), is associated with a mode of strong local free surface oscillation which decays slowly to infinity due to wave radiation.

For the ka=1.209, $\beta = 0°$ case the general response pattern is very similar for the two cases. There is an increase in the maximum run-up from 2.29 to 2.37 as shown in Figure 4 and there is a tendency for the patterns to focus around the flat faces. Figures 5(a) & 5(b) show that the flat faces cause an increase in amplification for several column diameters upstream of the structure.

For the $\beta = 45°$ cases the general response patterns are again quite similar but there are several small changes. For the non-circular case there is reduced run-up on the upstream and downstream columns but increased run-up on the two side columns. The maximum value anywhere in the field is 2.73 on the leading edge of the downstream column for the circular case but 2.69 on the inside faces of the side columns for the non-circular case, giving a small decrease in magnitude. As with the $\beta = 0°$ the flat faces tend to cause locally increased amplification and the pattern directly upstream of the leading column tends to be increased compared with the circular geometry. Amplification within the centre of the array is mostly decreased except for one peak near the centre that is increased. The risers and drilling equipment for a four column TLP or semi-submersible are often located in the centre of the structure. Therefore for design, run-up on the columns may be less of a problem than central upwelling.

4 CONCLUSION

Numerical analysis of run-up on single and square arrays of bottom-seated columns with varying cross-sectional shape but constant area was carried out. The final asymptote of the maximum run-up on the single cylinders is 2 for all cases.

Fresnel diffraction effects for the non-circular shaped cases cause the maximum run-up to rise well above this value before settling and also leads to significant variation along the faces of the columns. The field plots of maximum upwelling show changes in both position and amplitude of amplification peaks dependent on the column shape. This may have important implications for TLP and semi-submersible design.

Acknowledgement

The authors would like to thank EPSRC and BP for their funding of the CASE award to JRG.

5 REFERENCES

Evans D.V. & Porter R. (1997) Near-trapping of waves by circular arrays of vertical cylinders. Applied Ocean Research 19:83-99

McIver P. (1984) Wave forces on arrays of floating bodies. J Eng Maths 18:273-285

Molin B., Jamois E., Lee C.H., Newman J.N. (2005) Non-linear wave interaction with a square cylinder. Proc. 20th Int. Workshop Water Waves & Floating Bodies. Longyearbyen

Molin B., Remy F., Kimmoun O. (2007) Second-order wave interaction with a vertical plate. J Eng Math 58:109-119

Walker D.A.G., Eatock Taylor R., Taylor P.H. & Zang J. (2008) Wave diffraction and near-trapping by a multi-column gravity-based structure. Ocean Engineering 35(2):201-229